"Convection Jump" as a Subtropical Convergence Zone

*Naoki Sato[1], Masaaki Takahashi[2,3]
(1: IORGC, JAMSTEC, 2: CCSR, University of Tokyo and 3: FRCGC, JAMSTEC)
* Naoki Sato, IORGC, JAMSTEC, Japan, 237-0061, Natsushima-cho, Yokosuka, Japan.
e-mail: naoki@jamstec.go.jp

Abstract

Characteristics of the precipitation system corresponding to the "convection jump" were examined by analyzing observational data, focusing on the dynamical structure and the humidity gradient as well as the horizontal distribution of convective activity. As a result, a convection zone extending northeastward from the warm pool near the Philippines (hereafter called "Marcus Convergence Zone (MCZ)") was detected in late July. The horizontal distribution and rapid seasonal march of the convective activity do not directly correspond to those of sea surface temperature (SST). The distributions of sea level pressure, vorticity and vorticity budget well resemble those of a subtropic convergence zone (STCZ) revealed by previous studies. However, the gradient of precipitable water around the MCZ is not clear. Rather, it is implied that more water vapor exists on the northwestern side of the convergence zone.

Keyword: STCZ, convection jump, Baiu.

1. Introduction

Most of the precipitation during the Baiu period is brought by the Baiu frontal zone (BFZ). The midsummer season in Japan begins after an abrupt end of the Baiu rainy season. As for the relation between the convective activity in the low latitudes and the end of the Baiu, Ueda et al. (1995) pointed out that strong convective activity over the subtropical western North Pacific (WNP) which appears in late July causes an anticyclonic circulation on its northern side. Ueda et al. (1995) named this convective activity "convection jump". It appears that the warm SST over the WNP is one of the necessary condition for strengthening the convective activity. However, the spatial distribution of convective activity do not well correspond to that of SST. According to Ueda and Yasunari (1996), the years with typical convection jump are actually characterized by a positive SST anomaly over the subtropical WNP, which appears in early July. However, the positive SST anomaly is already weakened in late July in average. It seems difficult to explain the formation mechanism of the active convection only by the variation of the local SST.

On the other hand, Kodama (1992) examined properties of the precipitation systems over the low-latitude ocean, and showed that there exist three subtropical convergence zones (STCZs) such as the BFZ, the South Pacific Convergence Zone (SPCZ), and the South Atlantic Convergence Zone (SACZ). These STCZs can be regarded as rainfall belts which extend northeastward (southeastward) from the regions with strong diabatic heating associated with convective activity in the low latitudes in the Northern (Southern) Hemisphere. Kodama (1992) showed that the water vapor supply to the STCZs is contributed by the eastward flow along the front and the poleward one along the northwestern (southwestern) edge of the subtropical high. Furthermore, Kodama (1993) demonstrated that the existences of a subtropical jet and a low-level poleward flow along the western edge of the subtropical high are necessary to maintain the quasi-stationary precipitation zone. Kodama (1999) then showed that the formation of an STCZ is contributed by diabatic heating over the warm pool southwest of it, by numerical simulations utilizing an aqua-planet atmospheric general circulation model (AGCM).

From the above results, it is suggested that the convection jump may be an STCZ, since a warm pool and the Intertropical Convergence Zone (ITCZ) actually exist just to the southwest of the convection jump. In fact, the convection region shown by Ueda et al. (1995) and Ueda and Yasunari (1996) stretches northeastward. However, Ueda et al. (1995) and Ueda and Yasunari (1996) did not discuss the detailed structure of the convection jump or its relation to the convective activity to the southwest of it.

Therefore, in the present study, the structure of the convection jump is examined by analyzing observational data, considering a possibility that it is an STCZ simulated by Kodama (1999). We focus on the spatial structure rather than the fast seasonal march in the present paper. Equivalent black body temperature (T_{BB}), total precipitable water measured by Special Sensor Microwave/Imager (SSM/I), and objectively analyzed data are utilized for analyses in the following sections.

2. Methods

The horizontal distribution of convective activity is firstly examined by using T_{BB} data edited by the Meteorological Research Institute/Japan Meteorological Agency (MRI/JMA). The T_{BB} distributions in middle July (11–20 July) and late July (21–31 July) are examined. The difference between them is focused on, since the convection jump is observed in late July according to Ueda et al. (1995) and Ueda and Yasunari (1996). The averaged values for 18 years from 1980 to 1997 are analyzed.

Years 1983, 1984 and 1994 are selected as typical years when the low T_{BB} region corresponding to the convection jump in late July is especially clear. In the followings, analyses are performed for the three typical years, in order to clearly demonstrate the dynamical structure.

The composite distribution of T_{BB} in late July is firstly examined. Then, the composed 200 hPa geopotential height and sea level pressure (SLP) are calculated for the same period by utilizing objectively analyzed data by the National Centers for Environmental Prediction and the National Center for Atmospheric Research (NCEP/NCAR). The relative vorticity and the vorticity budgets (zonal advection, meridional advection and

stretching) for the 11-day averaged fields at 200 hPa and 850 hPa are also analyzed. Here, we focus on whether the dynamical features of an STCZ revealed by Kodama (1999) are identified for the convection jump or not.

The water vapor distribution is then examined. The total precipitable water by SSM/I is analyzed here. In this analysis, only data for 1994 are used, since data are not available until 1987.

3. Results

The T_{BB} distributions in middle and late July averaged from 1980 to 1997 are firstly examined. A low T_{BB} region runs from southwest to northeast around Marcus island can be seen only in late July. It is understood that the convective region extends northwestward from the warm pool. Although this result does not conflict with that shown by Ueda et al. (1995), we focus on the horizontal distribution of the convective area in more detail here. The convective region is stretched in a southwest-northeast direction. The southwestern part of the low T_{BB} region is accompanied by high SST (not shown). However, the northeastern part of the convective region does not corresponds to high SST. Further, there is no rapid seasonal march from middle to late July in the SST distribution. It should be noted that the spatial distribution and the seasonal changes in convective activity do not directly correspond to those in SST.

Figure 1 (upper) then shows the T_{BB} distributions in late July averaged for the selected typical years (1983, 1984, and 1994). It is clearly understood that the convective region extends northeastward from the warm pool around the Philippines. This horizontal structure of the convective region is similar to that simulated by Kodama (1999). It is also confirmed that the abrupt seasonal march occurs in middle or late July in typical years, as it does in the climatological mean field.

The composite wind vector at 850 hPa is shown in the lower panel of Fig. 1. Southerly wind is seen corresponding to the low-T_{BB} region in the upper panel. Comparing with those in Kodama (1992) and Kodama (1999), the wind direction is a little different. The southeasterly component is larger in Fig. 1 (lower), while southwesterly is dominant in the other STCZs shown in Kodama (1992) and Kodama (1999). The strong low-level southeasterly wind on the southeastern side of the low-T_{BB} region appears to be related to the large-scale anticyclonic circulation around the North Pacific subtropical high.

Figure 2 shows the 200 hPa geopotential height and SLP averaged for late July of the typical years. When we look at the large-scale features, we found that an upper-level anticyclone is located to the west of the convective area, accompanied by the strong diabatic heating over the Tibetan Plateau (the upper panel of Fig. 2). Further, a trough and a ridge are respectively identified on the northwestern and southeastern sides of the convection belt. In the lower layer, on the other hand, a trough is formed just near the convective area (the lower panel of Fig. 2). Corresponding to these results, an upper-level cyclonic vorticity anomaly is detected to the northwest of the low T_{BB} region, while an anticyclonic one is over and just to the southeast of it. A cyclonic relative vorticity is also confirmed in the lower layer in the convection zone

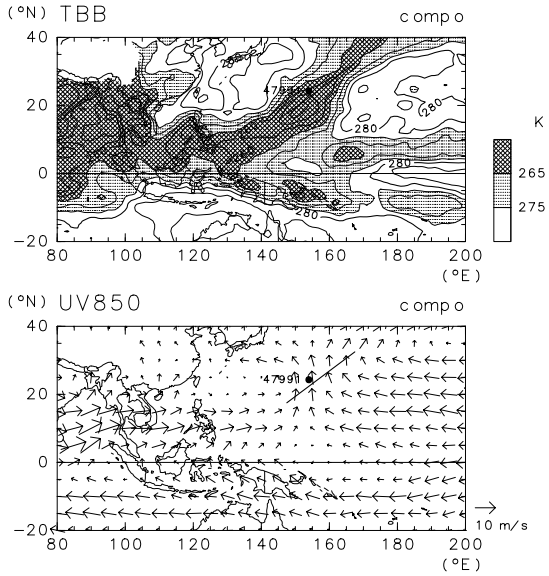

Fig. 1: T_{BB} (upper) and wind vector at 850 hPa (lower), averaged for late July (21–31 July) of 1983, 1984 and 1994. The contour interval is 5 K. The solid line in the figure indicates an approximate location of the convective region. The dot marked "47991" indicates the position of Marcus island.

(not shown).

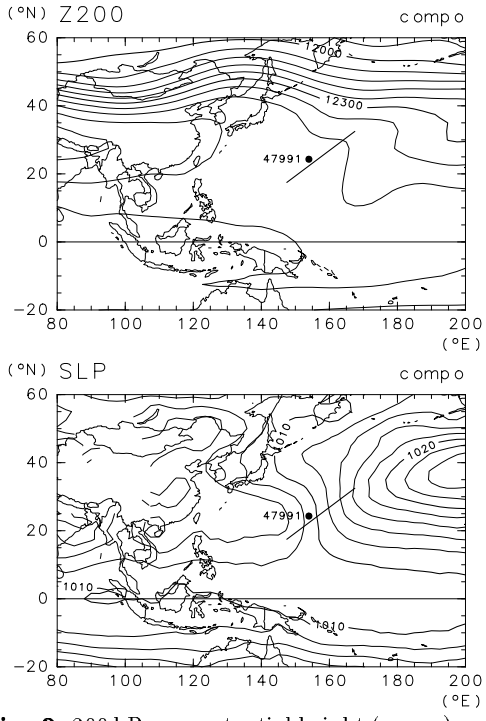

Fig. 2: 200 hPa geopotential height (upper) and SLP (lower) averaged for late July of 1983, 1984 and 1994. The contour intervals are 30 m and 2 hPa.

Then, the vorticity budget at the 200 hPa level in late July of the typical years is shown in Fig. 3. Note that the budget is calculated for the time-averaged field, and the feedback from transient eddies is neglected here. The upper, middle, and lower panels of Fig. 3 respectively indicate the zonal advection of vorticity, the meridional advection of absolute vorticity, and the stretching. A negative (anticyclonic) vorticity tendency brought by the stretching term is estimated over the convective area (the lower panel of Fig. 3). It appears that the zonal advection cancels the stretching term to the north of 30°N (the upper

panel of Fig. 3), and the meridional advection does to the south (the middle panel of Fig. 3). Figure 4 shows the vorticity budget at the 850 hPa level, as Fig. 3 does at the 200 hPa level. The contribution of the zonal advection is relatively small in the lower layer (the upper panel of Fig. 4). The positive stretching term corresponding to upward motion is balanced by the negative meridional advection term brought by southerly wind (the middle and lower panels of Fig. 4). This balance can be understood as the Sverdrup balance.

The SSM/I total precipitable water in late July of 1994 is shown in Fig. 5. More precipitable water is detected on the northwestern side of the rain belt rather than on the southeastern side. This gradient of precipitable water is especially clear to the north of 25°N. The result shown in Fig. 5 implies that the specific humidity in the lower layer is larger on the northwestern side, since most of the atmospheric water vapor exists in the lower troposphere. In general, a large value of time-averaged precipitable water which exceeds 40 mm is rarely observed in the mid- and high-latitudes (not shown). Thus, the large precipitable water observed to the northwest of the rain belt is a remarkable feature.

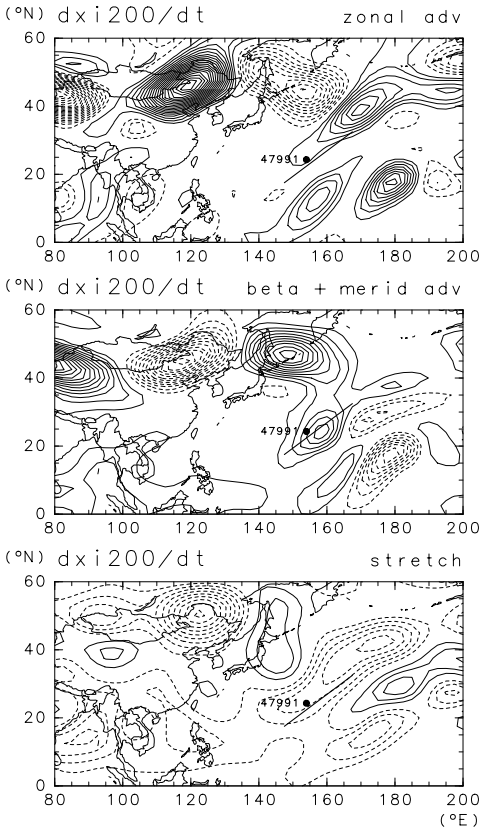

Fig. 3: Zonal advection of vorticity (upper), meridional advection of absolute vorticity (middle), and stretching term (lower) at 200 hPa averaged for late July of 1983, 1984 and 1994. The contour interval is $5\times10^{-11}\,s^{-2}$. The zero contour is suppressed, negative contours are dotted.

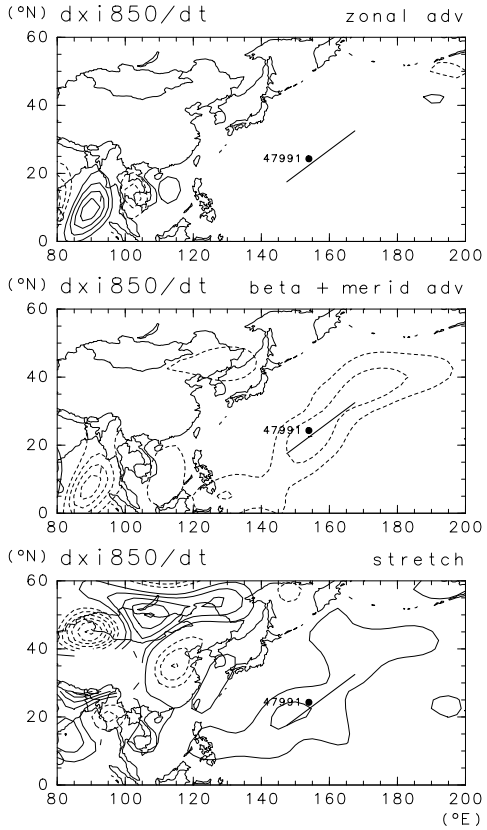

Fig. 4: The same as Fig. 3, except for 850 hPa.

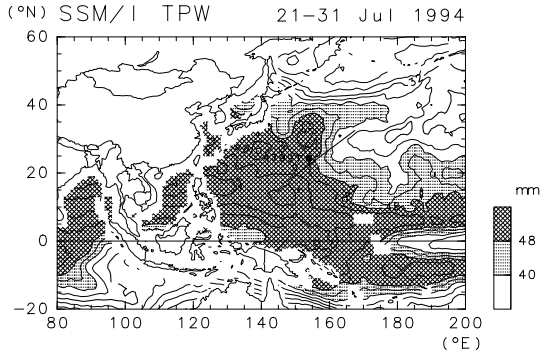

Fig. 5: Total precipitable water measured by SSM/I, in late July of 1994. The contour interval is 4 mm.

4. Discussion

As shown in Fig. 1 (upper), a convection region extending northeastward from the warm pool in the WNP is identified in late July, corresponding to the convection jump. The horizontal distribution of convective activity well resembles those in the observational results on STCZs by Kodama (1992) and the numerical one by Kodama (1999). Concerning the horizontal structure, the convection jump has common characteristics with the STCZs. Hereafter, we call the convergence zone the "Marcus Convergence Zone (MCZ)". In more detail, two separated minima of T_{BB} can be seen just near the Philippines and around 150°E in Fig. 1 (upper). Although such separated peaks of convection are not clear in the other observed STCZs, Kodama (1999) obtained a horizontal structure of rainfall which is somewhat similar to that of the MCZ shown in Fig. 1 (upper), in the numerical experiment. However, the formation mechanism of such double-peak structures are not yet revealed in Kodama (1999) and the present work. At least, it seems that the SST distribution can not directly explain the double-peak structure (not shown).

The rain belt is located to the northeast of a global-scale upper-level anticyclone shown in Fig. 2 (upper). By focusing on more detailed structure near the convection zone, we can see that a trough is formed to the northwest of the axis of the precipitation zone, and a ridge is to the southeast. According to the results of vortcity budget analysis in the upper layer, the zonal advection term and the effective β-term are canceled by each other on the subtropical jet located at 40–50°N, except near the precipitation zone (the upper and middle panels of Fig. 3). It implies propagation of a stationary Rossby wave. On the other hand, the contribution of the stretching term is not negligible (the lower panel of Fig. 3). It is inferred that vorticity forcing is imposed by convective activity. The upper-layer trough and ridge just near the precipitation zone can be interpreted as ones formed as a result of the balance between the stretching term and the other two terms of zonal advection and effective β-term. In the lower layer, cyclonic relative vorticity is generated just over the region with active convection, as shown in Fig. 2 (lower). The contribution of zonal advection of relative vorticity is negligible (the upper panel of Fig. 4), since zonal wind is weak in the lower layer (not shown). Fig. 4 (lower) indicates that positive vorticity forcing is brought corresponding to upward motion associated with convective activity. The vorticity forcing is balanced by effective β-term estimated in Fig. 4 (middle). Associated with this balance, southerly wind is analyzed in the lower layer (not shown). Although the southeasterly wind as a part of the anticyclonic circulation around the subtropical high is stronger than the other STCZs, the dynamical features of the MCZ discussed in this paragraph is basically consistent with those simulated by Kodama (1999). From a dynamical point of view, the authors think that the MCZ or the convection region associated with the convection jump can be regarded as an STCZ.

According to the SSM/I observation, the value of total precipitable water is larger on the northwestern side of the MCZ (Fig. 5), while it is larger on the low-latitude side of the other STCZs. At this point, the MCZ is quite different from the other STCZs. The gradient of precipitable water across the convergence zone is especially clear to the north of 25°N. Such a significant specific humidity gradient that more water vapor exists on the low-latitude side as is observed in the other STCZs does not exist around the MCZ. Some direct in-situ measurements, as well as further collection of observed data, will be required in the future works in order to reveal the water vapor distribution in more detail.

The smaller value of precipitable water in the southeastern side may correspond to the subsidence in the subtropical high. A dry region is also formed on the southeastern side of the convergence zone in the experiment by Kodama (1999). Kodama (1999) mentioned the possibility that the dry region is formed by the downward wind associated with the rain belt. It is still uncertain whether the dry air formation in the MCZ is contributed only by the downward motion related to the large-scale subtropical high. In a larger-scale field, the large value of precipitable water to the northwest of the MCZ is remarkable. The high concentration of water vapor seems to be brought by low-level wind around the thermal low over the continent and the moist tongue associated with the BFZ (Akiyama 1973). It is probably concluded that the specific humidity gradient, which may characterize the MCZ as a frontal zone, is formed by both the moist lower flow related to the BFZ, and the dry southerly wind along the western edge of the large-scale subtropical high.

The Sverdrup balance is established in the lower layer in and around the precipitation region associated with the MCZ, as shown in Fig. 4 (middle and lower). In other words, the lower southerly wind is observed corresponding to the upward motion. The MCZ is basically the same as the other observed STCZs at this point. However, the meridional gradient of specific humidity may be opposite to those of the other STCZs, as is inferred from Fig. 5. In such a condition, the southerly wind probably have negative effect on water vapor supply for the MCZ, although it advects moist air in the other STCZs. This negative feedback may be related to the observational fact that the duration of the MCZ is shorter than those of the others. Although a small dry region is also simulated in the aqua-planet experiment by Kodama (1999), its influence on the STCZ is not discussed in detail. We have to quantitatively understand the specific humidity and surface wind over the ocean, as well as the vertical wind, the surface latent heat flux and so on, in order to analyze moisture budget related to the MCZ.

5. Conclusions

Characteristics of the precipitation system related to the convection jump was examined, so that the "Marcus Convergence Zone (MCZ)" was identified as a convective region extending northeastward from the warm pool near the Philippines. The spatial distribution and temporal variations of convective activity do not directly correspond to those of local SST.

The dynamical properties of the MCZ represented by the pressure and vorticity distributions and the vorticity budget closely resemble those of the other observed STCZs and the simulated one in an AGCM. It can be concluded that the trough associated with the MCZ is formed by dynamical forcing related to active convection over the warm pool near the Philippines.

The distribution of water vapor around the MCZ is quite different from those around the other observed STCZs. It is implied that there exists more water vapor on the northwestern side of the convergence zone, supplied by the moist low-level southwesterly to the south of the BFZ.

References

Akiyama,*Pap. Met. Geophy.*, **24**, 157-188, 1973.
Kodama, *JMSJ*, **70**, 813-836, 1992.
Kodama, *JMSJ*, **71**, 581-610, 1993.
Kodama, *JAS*, **56**, 4032-4049, 1999.
Ninomiya, *JMSJ*, **62**, 880-894, 1984.
Ueda et al, *JMSJ*, **73**, 795-809, 1995.
Ueda and Yasunari, *JMSJ*, **74**, 493-508, 1996.